ELSEVIER

Catalysis Today 85 (2003) 49–57

CATALYSIS TODAY

www.elsevier.com/locate/cattod

Non-toxic Fe-based catalysts for styrene synthesis The effect of salt precursors and aluminum promoter on the catalytic properties

Alcinéia Conceição Oliveira [a], José L.G. Fierro [b], Antoninho Valentini [a], Paulo Sérgio Santana Nobre [a], Maria do Carmo Rangel [b,*]

[a] *Instituto de Química, Universidade Federal da Bahia, Campus Universitário de Ondina, Federação, 40 290-170 Salvador, Bahia, Brazil*
[b] *Instituto de Catalisis y Petroleoquímica, CSIC, Campus UAM, Cantoblanco, 28049 Madrid, Spain*

Abstract

The catalytic dehydrogenation of ethylbenzene to produce styrene is an important industrial process because it is used in the manufacture of resins, synthetic rubber and plastics. The most used catalysts for this process are iron oxides containing potassium and chromium oxides. These catalysts show high activity and selectivity but deactivate with time on-stream in the industrial units, mainly due to the loss of potassium. On the other hand, the storage of the exhausted catalytic materials causes environmental damage because of the toxicity of chromium compounds. In order to find non-toxic and potassium-free catalysts, the effect of aluminum and the salt precursor on the properties of iron oxides was investigated in this work. The catalysts showed high specific area, were resistant to reduction and were potassium-free; these features can prevent their deactivation. Also, they showed higher activity and selectivity than hematite and were no harmful for the environment. In these catalysts aluminum acts both as textural and structural promoter. Among the starting salt precursors studied (nitrate, sulfate and chloride), the iron chloride was the most efficient one, producing active and selective catalysts with high resistance against deactivation.

Keywords: Non-toxic catalyst; Ethylbenzene; Styrene

1. Introduction

Styrene is by far the most important member of a series of unsaturated aromatic monomers. It is used extensively for the manufacture of plastics, including crystalline polystyrene, rubber-modified impact polystyrene, acrylonitrile–butadiene–styrene (ABS) terpolymer, styrene–acrylonitrile (SAN) copolymer and styrene-butadiene rubber (SBR) [1].

The catalytic dehydrogenation of ethylbenzene in the presence of steam is the main commercial route for styrene production [2–5]. The reaction conditions are severe with a 873 K temperature and a gas phase at 1 atm of typically 12:1 (molar ratio) water-to-ethylbenzene depending slightly on the catalyst and on the process used [6]. The overall reaction is highly endothermic, reversible and equilibrium limited. Steam provides heat for the reaction and prevents over-reduction of the iron-based catalyst as well as coke formation. It also decreases the partial pressure of gases and thus shifts the chemical equilibrium to higher styrene conversion [2–4].

The most widely used industrial catalysts comprise iron oxide, potassium carbonate and promoters such

* Corresponding author.

0920-5861/$ – see front matter © 2003 Elsevier B.V. All rights reserved.
doi:10.1016/S0920-5861(03)00193-7

as chromium, cerium, molybdenum and vanadium oxides among others [4]. Other promoters like aluminum, cadmium, magnesium, manganese, nickel, uranium and rare earth have been used with and without vanadium [7]. Molybdenum and tungsten oxides have also been added to the catalyst [8]. However, potassium-promoted iron oxide is uniquely better than any other catalyst known for ethylbenzene dehydrogenation in the presence of steam [2,3]. It is generally accepted that potassium acts as a chemical promoter in the catalyst, whereas chromium oxide is a textural promoter stabilizing the high specific area of the active phase [2–4]. The reason for the effects of potassium promoter is not completely understood, although some insights into the reasons have been gained [9,10]. Some authors proposed that the function of potassium on the surface is to prevent the deactivation of the catalyst from coke formation [11] while others suggested that the active phase is a ternary metastable iron–potassium oxide with a loose platelet morphology which allows rapid transport of the gaseous reagents [6].

Although the commercial catalysts are very active and selective, they have some disadvantages: (i) the active oxidation state is unstable; hematite (α-Fe_2O_3) is preferred for styrene production, but tends to lower oxides and even to elemental iron, both of which catalyze carbon formation and dealkylation [3,4]; (ii) the catalysts have low specific area and (iii) they deactivate with time being susceptible to poisoning by halides and residual organic chloride impurities [2]. The most serious deactivation is caused by the loss of potassium promoter, which migrates in two directions as the catalyst ages. Potassium chloride is found downstream in the water layer of the condensed product as well as in catalyst pellets. In fact, a major migration of potassium occurs within the catalyst pellets, because the center of the pellets operates at a slightly lower temperature than the periphery due to the endothermicity of the reaction. Then the slight vapor pressure of the migrant form of potassium causes a shift of potassium toward this relatively cold center. In addition, potassium migrates also to the cooler part of the reactor (exit) [2–4]. Other disadvantages include the large amounts of steam used in industrial units increasing the operational costs. Also, the toxicity of the chromium compounds causes damage to the humans and to the environment [2,4]. Therefore, the investigation for new systems which have high specific areas and can stabilize the trivalent state of iron, in the absence of potassium, is much needed. Considering these aspects, the preparation of iron oxide-based catalysts, doped with aluminum and without potassium and chromium, was studied in this work. The effect of the salt precursor as well as the aluminum amount was also investigated in order to find the best method to prepare efficient catalysts. Aluminum has been proved an excellent promoter preventing sintering in iron-based catalysts [12,13]. On the other hand, the starting materials can play a significant role in the catalytic performance as stated before [14].

2. Experimental

2.1. Catalyst preparation

Reagents used were analytical grade. The catalysts were prepared by precipitation techniques at room temperature, followed by heating at 973 K for 2 h under nitrogen flow. Three kinds of salt precursors were used: (i) iron nitrate; (ii) iron sulfate and (iii) iron chloride. The iron-to-aluminum molar ratio was kept constant (5 and 10). Reference aluminum-free samples were also prepared, following the procedure described elsewhere [14].

In the sample preparation, an aqueous solution of iron nitrate (1N) and aluminum nitrate (0.1N) and a concentrated (25% (w/w)) aqueous solution of ammonium hydroxide were added to a beaker with water. The final pH was adjusted to 11 and the system was kept under stirring for additional 30 min. The sol produced was centrifuged (2000 rpm, 5 min) followed by a water rinsing to remove the nitrate ions from the starting material and centrifuged again. This procedure was repeated six times and the gel was dried in an oven at 393 K. The solid thus obtained was crashed, sieved in 100 mesh and then calcined at 973 K under nitrogen flow (60 ml min^{-1}), for 2 h. The same method was followed to prepare samples from iron chloride and iron sulfate.

2.2. Catalyst characterization

The qualitative analysis of nitrate was performed by adding about 1 ml of concentrated sulfuric acid to

10 ml of the liquid after centrifugation. The formation of $[Fe(NO)]^{2+}$ was detected by a brown ring [15]. The presence of nitrate, sulfate or chloride in the solids was detected by infrared spectroscopy in the range of 4000–650 cm^{-1} using a model IR-430 Shimadzu spectrometer and KI discs.

The iron and aluminum contents were determined by inductively coupled plasma atomic emission spectroscopy (ICP/AES) by using an Arl 3410 model machine. In the case of the samples prepared from iron chloride a Spectra AA-220 model Varian atomic absorption spectrometer was used instead, because of the interference of the chloride ions [16].

X-ray diffractograms were recorded at room temperature with a Shimadzu model XD3A instrument using Cu Kα radiation generated at 30 kV and 20 mA. The specific area (BET method) was measured in a Micromeritics model TPD/TPO 2900 equipment on samples previously heated under nitrogen (423 K, 2 h). The temperature programmed reduction (TPR) was performed in the same equipment, using a 5% H_2/N_2 mixture, from the room temperature to 1273 K.

X-ray photoelectron spectra were recorded in a VG ESCALAB 200R spectrometer equipped with a Mg Kα X-ray radiation source ($h\nu = 1253.6$ eV) and a hemispherical electron analyzer. The powder samples were pressed into small stainless steel cylinders and mounted onto a manipulator which allowed the transfer from the preparation chamber into the spectrometer. Before the analysis, they were outgassed (10^{-9} mbar) at 773 K for 1 h. The Al 2p peak (BE = 74.5 eV) was chosen as an internal reference. This reference was in all cases in good agreement with the BE of the C 1s peak, arising from contamination, at 284.9 eV. This reference gave an accuracy of +0.1 eV.

2.3. Catalytic activity

The catalysts were evaluated using 0.3 g of powder within −50 and +325 mesh size, and a fixed-bed microreactor, providing there is no diffusion effect. All experiments were carried out under isothermal condition (803 K) and at atmospheric pressure, employing a steam-to-ethylbenzene molar ratio of 10. The reactor, containing the catalyst, was heated under nitrogen flow (60 ml s^{-1}) up to the reaction temperature. Then the feed was interrupted and the reaction mixture was introduced. The reaction mixture was obtained by passing a nitrogen stream through a saturator with ethybenzene and then through a chamber where it was mixed with steam. The gaseous effluent was collected in a condenser and the organic phase was analyzed by gas chromatography, using a CG-35 instrument.

After each experiment, the Fe(II) and Fe(III) contents in the catalysts were determined to follow the iron reduction under the reaction atmosphere. For the Fe(II) analysis, samples were dissolved in concentrated hydrochloric acid, under carbon dioxide atmosphere and then titrated with potassium dichromate [15].

3. Results and discussion

Table 1 shows the results of the analyses of iron and aluminum. It can be noted that the solids showed an aluminum-to-iron molar ratio close to the starting solution except the samples prepared from iron chloride. This is in agreement with previous works [14,17,18] according to which the different ions (mainly chloride) in the precursor change the precipitation conditions of the iron compounds. In this case, the presence of chloride ions influenced the precipitation of iron and aluminum compounds, both chemical and physically, changing the chemical composition of the solids as compared to the expected one.

The infrared spectra of the solids before calcination showed characteristic bands of nitrate (1384 cm^{-1}), sulfate (1385 cm^{-1}) and chloride (700 cm^{-1}) [19] besides the broad Fe–O absorption band below 800 cm^{-1}

Table 1
Elemental analysis results of pure iron oxide prepared from iron nitrate (N sample), iron chloride (C) and iron sulfate (S) and of aluminum-doped iron oxide obtained from iron nitrate (NA10, NA5), iron chloride (CA10, CA5) and iron sulfate (SA10, SA5)

Sample	%Fe (±0.05)	%Al (±0.03)	Fe/Al (molar) (±0.05)
N	71.32	–	–
NA10	64.04	3.21	10.00
NA5	48.43	5.47	5.00
C	71.73	–	–
CA10	47.23	2.10	9.15
CA5	44.39	5.93	2.54
S	72.03	–	–
SA10	66.43	5.93	10.00
SA5	48.57	6.48	4.83

The numbers 10 and 5 represent the different iron-to-aluminum molar ratios.

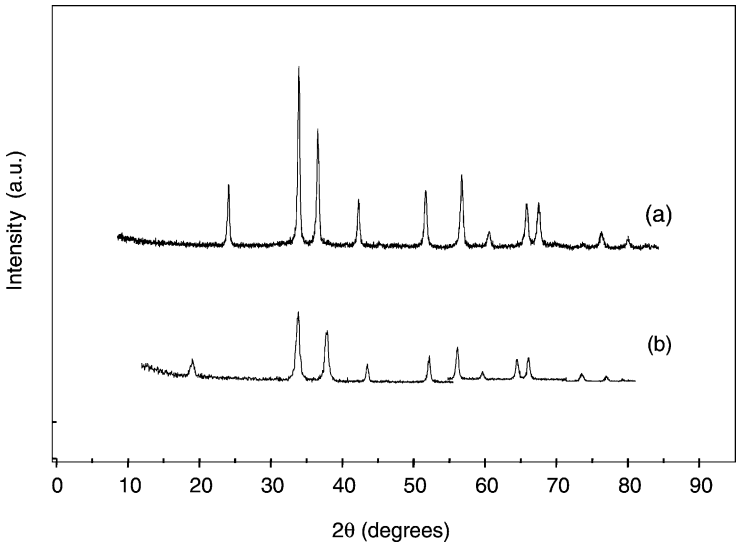

Fig. 1. X-ray diffraction patterns for the fresh (a) and used (b) catalysts (NA5 sample: aluminum-doped hematite prepared from iron nitrate with Fe/Al = 5).

[20]. After calcination, it was noted a strong decrease in the bands above 1000 cm^{-1}, showing that only small amounts of the anions remained in the calcined solids. The band below 800 cm^{-1} became narrower as a consequence of the iron oxide crystallization [20].

Hematite was found in the fresh catalysts and no change was noted due to the starting material or due to aluminum. Fig. 1 illustrates the typical X-ray diffraction pattern displayed by the samples. It can also be noted that aluminum did not significantly affect crystallization. No other phase besides hematite was detected. As aluminum has ionic radius similar to the iron atom, it is expected to go into the magnetite lattice [21] rather than to segregate as another phase. After the catalytic tests the catalysts showed the pattern of magnetite and hematite, as show in Fig. 1, independently of the starting material or the presence of aluminum.

The presence of aluminum increased the specific area of the fresh catalysts (Table 2), irrespective the salt precursor; this effect was lightly increased as the amount of aluminum increased in the solids, except in the case of the samples prepared from iron chloride. The same tendency was noted for the spent catalysts. These results are in accordance with previous works [13,22,23] about the role of aluminum as a textural promoter in several catalysts. This action has been traditionally associated with a surface phenomenon in which aluminum acts as a spacer, keeping the particles apart from each other [23]. However, Topsoe et al. [13] had shown that, in ammonia catalysts, a large fraction of aluminum is inside the iron particles as an occluded phase. Thus, aluminum causes strains in the lattice and shifts the equilibrium particle size toward smaller particles, since the ratio of strain to the surface effects becomes greater for larger particles.

Table 2
Surface area (S_g) of pure iron oxide prepared from iron nitrate (N sample), iron chloride (C) and iron sulfate (S) and of aluminum-doped iron oxide prepared from iron nitrate (NA10, NA5), iron chloride (CA10, CA5) and iron sulfate (SA10, SA5) before and after the catalytic tests

Sample	S_g ($m^2\,g^{-1}$) (fresh catalysts)	S_g ($m^2\,g^{-1}$) (spent catalysts)
N	17	11
NA10	57	24
NA5	60	28
C	5.0	5.0
CA10	6.0	5.0
CA5	22	5.5
S	12	12
SA10	25	25
SA5	28	28

The numbers 10 and 5 represent the different iron-to-aluminum molar ratios.

It can also be noted that the fresh samples prepared from iron nitrate have higher specific area than the other samples. As stated before [14], this can be explained by considering that the nitrate ions are the biggest ones and then generate more stresses in the lattice than the others. Therefore, they shift the equilibrium towards the smaller particles and decrease the ratio of strain to the surface. On the other hand, the chloride ions are the smallest ones causing less stresses and then did not increase the area so much [14]. The results of the present work showed that these effects also exist in the presence of aluminum and are, in fact, more important than aluminum in affecting the specific area of the solids. As a result of these effects, the NA5 sample showed the highest specific area while the C sample showed the smallest one.

During the catalyst test, the specific area of the aluminum-doped solids obtained from iron nitrate and from iron chloride decreased but those prepared from iron sulfate did not change. It shows that the compounds prepared from iron sulfate were more resistant to the coalescence of particles and pores that can occur during the transformation of hematite to produce magnetite [12]. As pointed out early [14], this can be explained by considering that, during the ethylbenzene dehydrogenation, a major fraction of the nitrate ions went away from the solid generating free volume and thus allowed it to sinter. On the other hand, sulfate ions are smaller than the nitrate ones and then the specific area was not so much affected. From the results of Table 2, one can note that aluminum also increased the specific area of the spent catalysts (obtained by both iron nitrate and iron sulfate) as occurred in the fresh ones. Concerning the samples prepared from iron chloride, a different behavior was noted. Aluminum increased the specific area of the fresh catalysts, specially the CA5 sample, but did not affect the spent ones. In the case of the CA5 sample, the higher area of the fresh catalyst (hematite) may be ascribed to the high amount of aluminum, in fact more aluminum than expected, as shown in Table 1. In the spent catalyst (magnetite), however, the chloride ions inhibit the action of aluminum as a textural promoter and this can be related to an interaction among aluminum and chloride ions, favored by the high amount of aluminum.

The TPR curves of the samples are shown in Fig. 2. They all showed similar profiles, with a peak at low temperatures (around 673 K), due to magnetite formation, and another one in the range of 873–1073 K, attributed to the formation of metallic iron [24], in accordance with previous work [14].

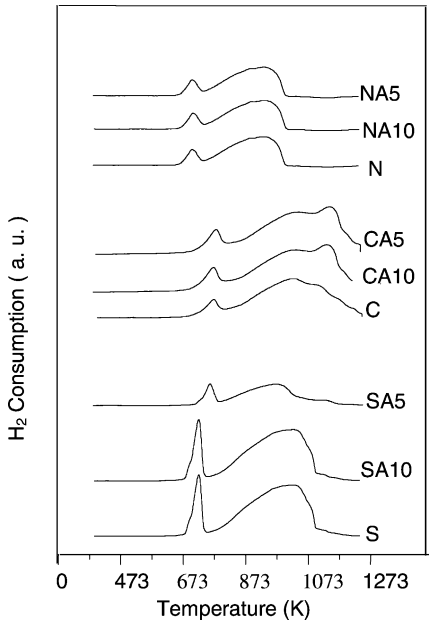

Fig. 2. TPR curves of pure iron oxide prepared from iron nitrate (N sample), iron chloride (C) and iron sulfate (S) and of aluminum-doped iron oxide prepared from iron nitrate (NA10, NA5), iron chloride (CA10, CA5) and iron sulfate (SA10, SA5). The numbers 10 and 5 represent the different iron-to-aluminum molar ratios.

In the aluminum-doped samples, the first peak was shifted to higher temperatures, as compared to aluminum-free solids, and this effect increased with the amount of aluminum in the samples. It means that aluminum makes the formation of magnetite more difficult. This temperature also varied with the salt precursor in the order C > S > N samples showing that iron chloride is the most appropriate salt precursor to prepare hematite resistant to reduction. The higher temperature peak was also affected. In the case of the catalysts prepared from iron sulfate, aluminum caused a decrease (in low amounts) or did not affect (in high amounts) the temperature, showing that it can prevent the over-reduction of iron. In the other cases, aluminum can prevent the production of metallic iron, since the peak was shifted to higher temperatures. Table 3 shows the temperatures related to magnetite and to iron metallic formation.

Table 3
Temperature of magnetite (T_m) and metallic iron (T_i) formation obtained from the TPR curves

Sample	T_m (K)	T_i (K)
N	653	883
NA10	656	891
NA5	660	893
C	685	1023
CA10	698	1016
CA5	723	1056
S	661	890
SA10	654	883
SA5	688	889

N, C and S samples: iron oxides prepared from iron nitrate, iron chloride and iron sulfate, respectively. NA10, CA10 and SA10 samples: aluminum-doped iron oxide obtained from iron nitrate, iron chloride and iron sulfate, respectively, with Fe/Al = 10. NA5, CA5 and SA5 samples: aluminum-doped iron oxide prepared from iron nitrate, iron chloride and iron sulfate, respectively, with Fe/Al = 5.

The hydrogen consumption in the TPR experiments are shown in Table 4. All samples showed a hydrogen consumption lower than the calculated value for hematite reduction to produce magnetite (73.2 μmol) and for magnetite reduction to produce metallic iron (816.5 μmol) considering the sample weight (0.035 g) used in the experiments. It shows that the reduction was not complete in the conditions of the experiments.

Table 4
Hydrogen consumption in the magnetite formation and in the metallic iron formation obtained from the TPR curves

Sample	H_2 consumption in the magnetite formation (μmol)	H_2 consumption in the metallic iron formation (μmol)
N	22.3	54.0
NA10	18.8	57.1
NA5	21.9	57.6
C	21.4	57.1
CA10	21.9	61.6
CA5	21.9	59.8
S	22.8	57.1
SA10	23.2	66.1
SA5	21.9	61.6

N, C and S samples: iron oxides prepared from iron nitrate, iron chloride and iron sulfate, respectively. NA10, CA10 and SA10 samples: aluminum-doped iron oxide prepared from iron nitrate, iron chloride and iron sulfate, respectively, with Fe/Al = 10. NA5, CA5 and SA5 samples: aluminum-doped iron oxide prepared from iron nitrate, iron chloride and iron sulfate, respectively, with Fe/Al = 5.

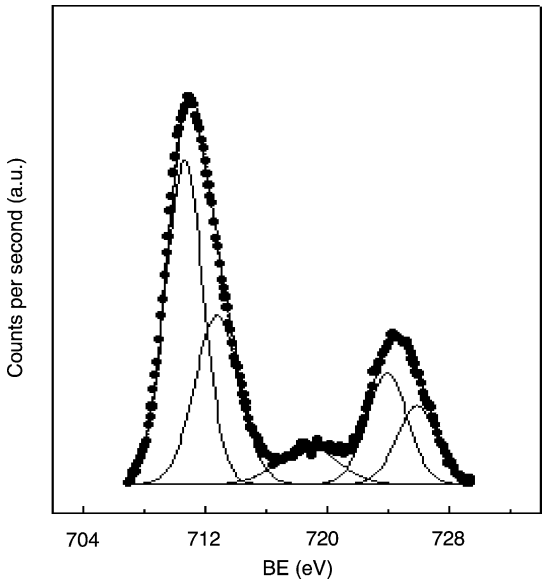

Fig. 3. Fe 2p core-level spectra for aluminum-doped iron oxide prepared from iron sulfate with Fe/Al = 5 (SA5 sample) before the catalytic test.

It can also be noted that the hydrogen consumption varies with the presence and the amount of aluminum in solids as well as with the starting materials. However, it is not possible to state a relationship among these values and the catalyst properties because the high temperature peak is broad suggesting that some magnetite was produced simultaneously with metallic iron.

A typical Fe 2p core-level spectrum of the catalysts before the reaction is shown in Fig. 3. A similar profile was got with spent catalysts. The Fe^{3+} species can be identified by a peak at around 710.0 eV, and a satellite structure located at the high binding energy side, which is characteristic of hematite [25]. Comparing this result with that obtained by X-ray diffraction, one can see that after the reaction the catalyst was made off hematite and magnetite but the catalyst surface was covered by hematite. This phase could not be identified by X-ray diffraction probably because the particles were too small or were present in very small amounts.

The binding energies (BE) of some characteristic core levels of Fe, Al, O, S and Cl in the samples are displayed in Tables 5 and 6. The binding energy for the Al 2p peak was in close agreement with that for Al^{3+} in $Al_2O_4^{2-}$ type compounds [25]. The presence

Table 5
Binding energies (eV) of iron oxide and of aluminum-doped iron oxide prepared from iron nitrate (N, NA10, NA5), iron chloride (C, CA10, CA5) and from iron sulfate (S, SA10, SA5) before the catalytic tests on samples previously treated under vacuum

Sample	Al 2p	Fe $2p_{3/2}$	O 1s	S 2p	Cl $2p_{3/2}$
N	–	711.3	532.6	–	–
NA10	74.4	710.5	530.1 (64) 532.0 (36)	–	–
NA5	74.4	710.6	530.0 (59) 532.0 (41)	–	–
C	–	711.5	532.6	–	–
CA10	74.5	710.5	529.9 (68) 531.8 (31)	–	–
CA5	74.5	710.5	529.9 (68) 531.8 (32)	–	198.2
S	–	711.5	532.6	168.7	–
SA10	74.4	710.7	530.0 (69) 531.9 (31)	168.6	–
SA5	74.5	710.6	530.1 (60) 532.1 (40)	168.7	–

The numbers 10 and 5 represent the different iron-to-aluminum molar ratios.

Table 6
Binding energies (eV) of aluminum-doped iron oxide prepared from iron nitrate (NA10, NA5), iron chloride (CA10, CA5) and iron sulfate (SA10, SA5) after the catalytic tests on samples previously treated under vacuum

Sample	Al 2p	Fe $2p_{3/2}$	O 1s	S 2p	Cl $2p_{3/2}$
NA10	74.4	710.5	530.4 (65) 531.9 (35)	–	–
NA5	74.5	710.6	530.4 (63) 532.0 (37)	–	–
CA10	74.5	710.3	530.2 (65) 531.9 (35)	–	–
CA5	74.5	710.4	530.2 (60) 531.9 (40)	–	198.1
SA10	74.5	710.5	530.3 (69) 531.9 (31)	–	–
SA5	74.4	710.4	530.3 (66) 531.9 (34)	–	–

The numbers 10 and 5 represent the different iron-to-aluminum molar ratios.

Table 7
Surface atomic ratios (Fe/Al, SO_4^{2-}/Fe and Cl^-/Fe) of aluminum-doped iron oxide prepared from iron nitrate (NA10, NA5), chloride (CA10, CA5) and sulfate (SA10, SA5) before and after the catalytic tests on samples previously treated under vacuum

Sample	Fe/Al	SO_4^{2-}/Fe	Cl^-/Fe
NA10 (fresh)	2.203	–	–
NA10 (spent)	0.826	–	–
NA5 (fresh)	0.853	–	–
NA5 (spent)	0.412	–	–
CA10 (fresh)	1.244	–	0.158
CA10 (spent)	0.605	–	0.246
CA5 (fresh)	1.047	–	0.245
CA5 (spent)	0.636	–	0.107
SA10 (fresh)	2.118	0.122	–
SA10 (spent)	0.881	–	–
SA5 (fresh)	0.945	0.202	–
SA5 (spent)	0.655	–	–

The numbers 10 and 5 represent the different iron-to-aluminum molar ratios.

of chloride and sulfate ions on the catalysts surface was detected by the binding energies at around 198.2 and 168.7 eV, respectively [25]. In all cases, the binding energies were essentially constant for the catalysts, regardless the presence of the promoter or the kind of the salt precursor. After the catalytic test, the peak related to sulfate species disappeared showing that they migrated from the surface during the reaction. The binding energies are similar in fresh and spent catalysts showing that the same species were present on catalyst surface in both cases.

The chemical state of the components and the relative concentration at the surface are shown in Table 7. It can be noted that the values of Fe/Al molar ratio on the catalyst surface are lower than that of the bulk catalyst (Table 1), which means that most of aluminum is present on the solid surface. Therefore, the role of aluminum in increasing the specific area of the catalysts seems to be related mainly to the action of aluminum as a spacer on the surface, rather than causing strains in the lattice. Also, it can be seen that more aluminum ions went to the solid surface during the reaction, as shown by the XPS results of the spent catalysts. The samples prepared from iron chloride showed chloride species on the catalyst surface also. By comparing the surface of the CA10 sample (Fe/Al = 10) and the surface of the CA5 sample (Fe/Al = 5), one can note that the small difference in the amount of aluminum

Table 8
Catalytic activity (a), activity per area (a/S_g) and selectivity (S) of pure iron oxide prepared from iron nitrate (N sample), chloride (C) and sulfate (S) and of aluminum-doped iron oxide prepared from iron nitrate (NA10, NA5), chloride (CA10, CA5) and sulfate (SA10, SA5) in the ethylbenzene dehydrogenation and the Fe(II) to Fe(III) molar ratio in the spent catalysts

Sample	a ($\times 10^4$ mol g^{-1} h^{-1}) ($\pm$0.1)	a/S_g ($\times 10^4$ mol g^{-1} m^{-2}) ($\pm$0.1)	Fe(II)/Fe(III) ($\pm$0.05)	Selectivity (%) ($\pm$0.1)
N	2.6	1.2	0.50	92.0
NA10	2.9	2.4	0.49	94.1
NA5	5.9	2.1	0.52	93.2
C	3.0	1.5	0.20	83.1
CA10	5.0	2.3	0.21	85.3
CA5	5.5	3.3	0.20	94.0
S	1.3	0.5	0.30	84.3
SA10	2.1	0.7	0.32	92.3
SA5	3.8	1.5	0.29	96.0

The numbers 10 and 5 represent the different iron-to-aluminum molar ratios.

can not justify the large difference in the specific areas. Therefore, a large contribution of the strains in the lattice, in favoring the production of small particles, is expected in the CA5 sample which has much more aluminum. During the reaction, the surface of both samples changed, due to the change phase from hematite to magnetite. This phase change seems to increase the interaction among aluminum and chloride ions, so that aluminum does not act as a textural promoter in the spent catalysts. On the other hand, the sulfate species were present only on the surface of the fresh catalysts, which means that they did not affect so much the mobility of the species.

All catalysts were active to the ethylbenzene dehydrogenation, as shown in Table 8. The definition of activity, used in this work, considers the number of moles of ethylbenzene that reacts per hour and per gram of catalyst. Aluminum led to an increase in activity and in activity per area and these effects increased with its amount in the solids. As the specific areas also increased due to aluminum, one can conclude that it acts both as textural and structural promoter. However, both effects depend on the salt precursors. The catalysts prepared from iron chloride were the most active and those prepared from iron sulfate were the least ones. The highest value of the activity per area was shown by the CA5 sample which is supposed to have a strong interaction among aluminum and chloride ions. This result suggests that when the chloride species went from the surface, during the magnetite formation, the iron species on the surface remained in a very active and selective state to styrene production. In all samples, the structural action of aluminum and the effect of the starting materials on the activity per area can be explained by considering that the Fe^{3+} species form the active phase in ethylbenzene dehydrogenation [2–4]. As shown by the XPS results, these species were stabilized on the catalyst surface, probably due to the action of aluminum in preventing the iron reduction.

The selectivity increased due to aluminum except in the samples prepared from iron nitrate. The definition of selectivity, used in this work, considers the number of moles of styrene produced per number of moles of ethylbenzene that reacted. The Fe(II)/Fe(III) molar ratios of the spent catalysts, prepared from iron nitrate, were closed to the stoichiometric value of magnetite (0.5) confirming that this phase was present in the solids. On the other hand, the spent catalysts obtained from iron sulfate and iron chloride were lower than this value showing that the Fe^{3+} species were more stabilized in these solids.

4. Conclusions

Aluminum-based iron oxides are efficient catalysts to the ethylbenzene dehydrogenation, with the advantage of being non-toxic for the environment. The catalyst surface is made off Fe^{3+} species which assures high activity and selectivity. Also, they are resistant to deactivation due to their high specific area, their resistance to reduction and the absence of potassium. In these catalysts aluminum acts both as textural and

structural promoter. Iron chloride is the most efficient salt precursor, as compared to iron nitrate and iron sulfate, producing active and selective catalysts with resistance against deactivation.

Acknowledgements

ACO acknowledges to CNPq his graduate fellowship. This work was done by grants from FINEP and CNPq.

References

[1] Kirk-Othmer, Encyclopedia of Chemical Technology, Willey, New York, 1984, p. 770.
[2] E.H. Lee, Catal. Rev. 8 (1973) 285.
[3] B.D. Herzog, H.F. Raso, Ind. Eng. Chem. Prod. Res. Dev. 23 (1984) 187.
[4] A.B. Styles, in: B.E. Leach (Ed.), Applied Industrial Catalysis, Academic Press, New York, 1983, p.137.
[5] S.S.E.H. Elsanashaie, B.K. Abdallah, S.S. Elshishini, S. Olkowalter, M.B. Noureldeen, T. Aboudani, Catal. Today 64 (2001) 151.
[6] M. Muhler, R. Schkogl, G. Ertl, in: Proceedings of the 9th International Congress On Catalysis, Calgary, Canada, 1988, p. 1758.
[7] G.H. Riesser, US Patent 4,152,300 (1979).
[8] G.H. Riesser, US Patent 4,144,197 (1979).
[9] E.H. Lee, L.H. Holmes Jr., J. Phys. Chem. 67 (1963) 947.
[10] A.K. Vijh, J. Chem. Phys. 72 (1975) 5.
[11] Z. Gao, B. Zhang, J. Cui, Appl. Catal. 12 (1991) 332.
[12] G.C. Araújo, M.C. Rangel, Catal. Today 62 (2000) 201.
[13] H. Topsoe, J.A. Dumesic, M. Boudart, J. Catal. 28 (1978) 477.
[14] A.C. Oliveira, M.C. Rangel, React. Kinet. Catal. Lett. 5 (2002) 135.
[15] A.I. Vogel, Quantitative Inorganic Analysis, Longman, London, 1961, p. 309.
[16] D.G. Chambaere, D. Grave, Phys. Stat. Sol. 12 (1989) 18.
[17] J. Livage, Catal. Today 41 (1998) 8.
[18] E. Matjievic, P. Sheider, J. Colloid. Interf. Sci. 63 (1978) 508.
[19] R.A. Niquist, R.O. Kagwel, Infrared Spectra of Inorganic Compounds, Academic Press, Orlando, 1971, p. 43.
[20] U. Schwertmann, W.R. Fischer, Geoderma 10 (1973) 237.
[21] M.E. Dry, L.C. Ferreira, J. Catal. 7 (1967) 352.
[22] J. Ladebeck, K. Kochloefl, in: G. Poncelet, et al. (Eds.), Sicentific Bases for Preparation of Heterogeneous Catalysts. Elsevier, Amsterdam, 1995, p. 1079.
[23] A. Nielsen, H. Bohlbro, An Investigation on Promoted Iron Catalysts for the Synthesis of Ammonia, Gjellerup Forlag, Copenhagen, 1968, p. 221.
[24] J.C. Gonzalez, M.G. González, M.A. Laborde, N. Moreno, Appl. Catal. 20 (1986) 3.
[25] C.D. Wagner, W.M. Riggs, L.E. Davis, J.F. Moulder, G.E. Muilenberg, Handbook of X-Ray Photoelectron Spectroscopy, Perkin-Elmer Coorporation, Eden Prairie, 1978, p. 76.